Ionization of rubidium by 50-eV electrons

M. A. Haynes,[1] B. Lohmann,[1] I. Bray,[2] and K. Bartschat[3]
[1]*Centre for Quantum Dynamics, Griffith University, Nathan, Queensland 4111, Australia*
[2]*Centre for Atomic, Molecular and Surface Physics, School of Engineering Sciences, Murdoch University, Perth 6150, Australia*
[3]*Department of Physics and Astronomy, Drake University, Des Moines, Iowa 50311, USA*
(Received 19 November 2003; published 16 April 2004)

We report on a joint experimental and theoretical study of 50-eV electron-impact ionization of rubidium. Comparison of the experimental data with theoretical predictions from various models shows good qualitative agreement, as long as distortion and channel-coupling effects in the projectile-target interaction are accounted for. The remaining differences between experiment and theory indicate the need for further studies of this collision system.

DOI: 10.1103/PhysRevA.69.044704 PACS number(s): 34.80.Dp

I. INTRODUCTION

The most complete information on the electron-impact ionization process is obtained by detecting, in coincidence, the scattered, and ejected electrons produced in the ionizing collision, the so-called $(e,2e)$ experiments [1]. In these experiments, the momenta of the incident, scattered, and ejected electrons are fully determined. This powerful technique has been applied to the investigation of this collision process for a wide range of targets. The first $(e,2e)$ measurements for electron-impact ionization of alkali metals were performed by Frost and Weigold [2] on sodium and potassium. These experiments are now classed as electron-momentum spectroscopy (EMS) experiments, designed to measure the electron-momentum density distribution of the atomic electrons. In EMS experiments, the two outgoing electrons from the ionization event are detected with equal energies, in a symmetric noncoplanar geometry. The measurements of Frost and Weigold were performed at relatively high incident energies, and the results were well described by a plane-wave impulse approximation calculation. In order to investigate the dynamics of the collision in more detail, it is generally necessary to employ other kinematic arrangements, and a wide range of geometries and energy regimes have been accessed in $(e,2e)$ experiments. Indeed the technology used in these experiments has evolved to the point where the spin of the electrons involved in the ionization process can also be determined. Recent coincidence measurements of electron-impact ionization of lithium and sodium employed spin-polarized electrons in a coplanar asymmetric geometry [3,4], and the results have offered a particular challenge to theorists. In Ref. [3] the experimental data were compared with two of the most sophisticated theoretical models available, the convergent close-coupling (CCC) method and the distorted-wave Born approximation (DWBA). Lower *et al.* [4] considered two approximations, the DWBA and the dynamically screened three-Coulomb-wave method. The comparison of theory and experiment showed varying levels of agreement with the different theoretical approximations, depending upon the kinematical regime under investigation, and the results clearly indicated that the most stringent test of the theories occurs for low incident and outgoing electron energies. As pseudo-one-electron targets, alkali-metal atoms offer an attractive test bed for theory, in particular, for computationally intensive calculations such as the convergent close-coupling approximation.

Here we present experimental and theoretical studies of the $(e,2e)$ process in rubidium. The experimental data have been acquired in the coplanar asymmetric geometry, in which the two outgoing electrons are detected with different energies and angles. The measurements were performed as a prelude to future experiments on laser-excited rubidium targets. The experimental results are compared with two theoretical calculations, one using the CCC method and the other a hybrid approach using a distorted-wave description for the "fast" projectile and an *R*-matrix (close-coupling) approach for the initial bound state and the ejected-electron–residual-ion interaction.

II. EXPERIMENT

The electron coincidence spectrometer used in the measurements is described in detail in Ref. [5], and hence we give only a brief overview here of the apparatus, albeit with somewhat more detail on those elements which have been added for the rubidium measurements. A schematic diagram of the apparatus is shown in Fig. 1.

Two hemispherical electron energy analyzers equipped with channel electron multipliers are used to analyze energy and detect the outgoing electrons from the ionization event. The geometrical acceptance angles of the two analyzers are ±1.5°. The analyzers are mounted on concentric independent turntables. The incident electron beam is produced by an electron gun with a thoriated tungsten filament, and the incident and detected electrons all lie in the same plane (the scattering plane). The rubidium target beam is produced by a resistively heated oven; the atom beam also lies in the scattering plane, and the intersection of the incident electron beam and the atom beam defines the interaction region. In the coplanar asymmetric geometry, the higher-energy outgoing electron (designated the scattered electron) is detected at a fixed forward angle, while the slower outgoing electron is identified as the ejected electron, and is detected over a broad angular range. Coincidence fast timing electronics ensure

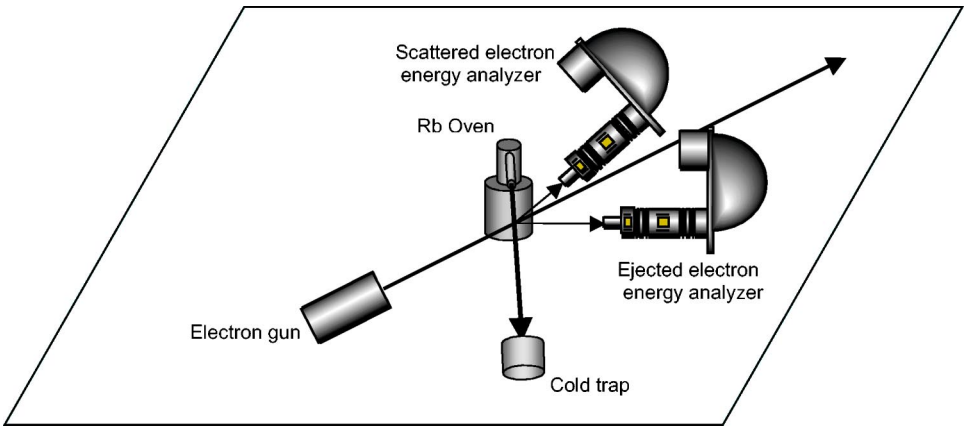

FIG. 1. Schematic diagram of the apparatus.

that pairs of electrons which do not originate from the same ionizing event are discriminated against. The coincidence energy resolution in these experiments was 0.9 eV.

The new rubidium oven is machined from stainless steel and is composed of two sections, the reservoir section and the nozzle section, with the two sections being sealed by a copper gasket. Both the reservoir and nozzle sections are wound with Thermocoax, and can be independently heated. During operation, the reservoir is maintained at a temperature of $\approx 200°$C, while the nozzle section is $\approx 60°$C higher in temperature. The rubidium beam exits the oven through a nozzle 40 mm long, with an internal diameter of 1 mm. After passing through the interaction region, the rubidium beam is deposited in a liquid-nitrogen-cooled cold trap, which is held at a temperature of $-55°$C. Although the cold trap removes the bulk of the rubidium vapor from the chamber, there is still rubidium deposition on various elements of the spectrometer, and this deposition can result in changing contact potentials within the system. Such changing contact potentials can produce shifts in the energy position at which the coincidence signal is found, thereby reducing the count rate. In order to ensure that the coincidence signal remained within the appropriate energy window during an experimental run (angular scan), the experiment had to be continuously monitored for periods of up to 18 h. The experiments were performed at an incident energy E_0 of 50 eV, ejected-electron energy E_2 of 10 eV, and scattered electron detection angles of $-15°$ and $-20°$.

The energy of the scattered electron (E_1) is determined by energy conservation,

$$E_0 = E_1 + E_2 + \varepsilon_i$$

where ε_i is the binding energy of the 5*s* electron in rubidium (4.18 eV). The accessible angular range of the ejected-electron energy analyzer is from +40° to +100°.

III. THEORY

A. The convergent close-coupling method

The CCC approach to electron-alkali-metal atom excitation has been detailed in Ref. [6], where excellent agreement with spin-resolved and superelastic electron-sodium data was presented on a broad range of energies. Similar high quality agreement was found with the data from superelastic electron scattering experiments with laser-excited lithium [7] and potassium [8]. However, the quality of the agreement has deteriorated somewhat when the target becomes as heavy as Rb [9]. The extension to ionization processes has been given initially by Bray and Fursa [10] and finalized recently by Bray [11]. Briefly, the alkali-metal atom is treated as a single valence electron moving in a frozen-core Hartree-Fock plus a phenomenological core-polarization potential. The target states are obtained by diagonalizing the target Hamiltonian in a Laguerre basis with parameters: the maximum orbital angular momentum l_{max}, the basis size N_l, and the exponential falloff λ_l. With increasing N_l the corresponding negative-energy states converge to the true eigenstates, while the positive-energy states provide for an increasingly dense discretization of the target continuum. While we are free to choose the parameters N_l and λ_l, in practice, we set $\lambda_l = \lambda$ to be a value such that convergence in the results of interest is obtained by taking a computationally practical value of N_l. Furthermore, we take $N_l = N_0 - l$, and thus have substantially reduced the total number of parameters to just three, l_{max}, N_0, and λ.

Since the ionization potential of Rb is relatively small, larger-l target states may be readily excited. This leads to major computational problems because of the number of channels $(l+1)$ such states generate. The present ionization kinematics are of the asymmetric energy-sharing type. The slow electron has 10-eV energy, and we find that $l_{max} = 10$ is necessary to get reasonable convergence with increasing l_{max}. Even larger l_{max} would be desirable, but are beyond our computational resources. Through a series of calculations we determined that a good choice for N_0 and λ are 40 and 6.04, respectively. The specific choice of 6.04 was arrived at after a slight variation around 6.0 to ensure no pseudothreshold at exactly the total energy E. Only one closed state was retained for each l. This resulted in a close-coupling calculation with 139 states and 745 channels that required 16 Gb of computer memory. Upon completion of the CCC calculation the ionization amplitudes are determined from excitation amplitudes of the positive-energy states as described by Bray and Fursa [10]. The incident energy of 50 eV is relatively large

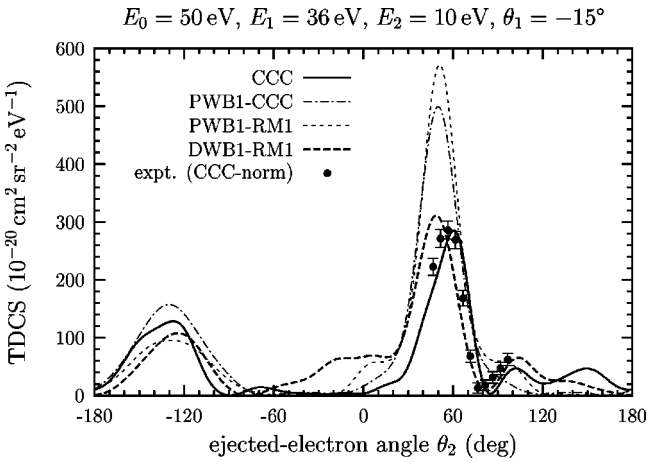

FIG. 2. Triple differential cross section for electron-impact ionization of Rb(5*s*) at an incident electron energy of 50 eV. The faster (scattered) outgoing electron with energy 36 eV is observed at a fixed angle of −15°, in coincidence with the lower (ejected) electron of energy 10 eV. The detection angle for the latter electron is varied. The experimental values are made absolute by normalizing the peak values to the CCC prediction. The PWB1-RM1 and DWB1-RM1 are described in the text, while PWB1-CCC represents the first-order plane-wave Born prediction from the CCC code.

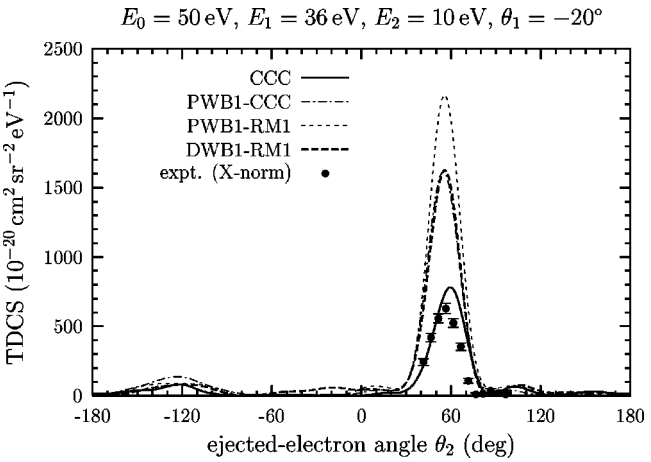

FIG. 3. Same as Fig. 2 for a scattering angle of −20°, except that the experimental data are now internormalized to the experimental values at −15°.

since it is more than ten times the ionization threshold. Consequently, the singly differential cross section (SDCS) is highly peaked for asymmetric energy sharing, and is particularly small for equal energy sharing, with the SDCS being free from oscillations that are evident at smaller incident energies [12]. The triply differential cross sections are generated directly from the ionization amplitudes and do not require any rescaling [13].

B. DWBA +*R* matrix

This method is based on the formalism outlined by Bartschat and Burke [14] and the computer program RMATRX-ION of Bartschat [15]. The basic idea is to describe a "fast" projectile electron by either a plane wave or a distorted wave and then calculate the initial bound state and the interaction between the residual ion and the "slow" ejected electron by an *R*-matrix (close-coupling) expansion. Although second-order effects in the projectile-target interaction can now be taken into account approximately [16,17], this was not done in the present work. Tests showed that evaluation of the second-order term may not be sufficiently reliable for the relatively low incident energy of 50 eV.

In order to highlight the importance of various physical effects and to complement the CCC calculation described above, we therefore used the simplest possible model, namely, a first-order plane-wave or distorted-wave representation for the projectile and a one-state (static-exchange) approximation for electron scattering from Rb^+. These models are labeled PWB1-RM1 and DWB1-RM1 below. A large number of partial waves (up to 90) for the fast projectile guaranteed the convergence of its partial-wave expansion, while similar problems as in the CCC calculation arose because of the high multipole components in the projectile-target interaction that lead to substantial contributions to the results also from high angular momenta of the ejected electron.

IV. RESULTS AND DISCUSSION

Figure 2 shows our first set of results for the triple differential cross section for electron-impact ionization of Rb(5*s*) at an incident electron energy of 50 eV, with outgoing electron energies of 36 eV and 10 eV, respectively, and observation of the faster of these two electrons at the fixed scattering angle of −15°. Since there are significant differences between the predictions obtained with the first-order plane-wave models for the projectile and the more elaborate calculations, we conclude that such a model is not sufficient for this case. Although this finding may not be surprising, the good agreement between the predictions from two very different implementations of these first-order models gives us confidence that the same basic physics is described in the rest of the problem, most importantly the initial state and the ejected-electron-residual-ion interaction.

Using either a first-order distorted-wave description of the projectile or the very large close coupling with pseudostates expansion in the CCC method drops the height of the binary peak by about a factor of 2 in this case. Since the experimental data are relative, we have normalized them here to the peak value of the CCC prediction.

Most interesting, however, is the fact that while CCC and DWB1-RM1 agree on the magnitude of this peak to within 10 %, CCC predicts the peak to move to the right from the momentum-transfer direction (which coincides with the peak position in the plane-wave models), while DWB1-RM1 predicts a slight shift to the left. Experimentally, the peak is indeed found to the right of the momentum-transfer direction, but not as far as predicted by the CCC calculation.

Figure 3 shows similar results for the larger scattering angle of −20°. In this figure, the experimental data have been cross normalized to the data at −15°, i.e., without further reference to theory. Because of the increase in scattering

angle, it is not surprising that the first-order plane-wave models are even less appropriate for this situation, at least with respect to the relative heights of the binary peaks. In this case, DWB1-RM1 has also become problematic in that it predicts too high a peak. As expected, the CCC model does best, although there is now a small disagreement between CCC and experiment in the peak height. Also, the predicted shift of the peak to the right is again not seen to the same extent in the experimental data.

V. SUMMARY AND CONCLUSION

We have presented first results from a joint experimental and theoretical study of 50-eV electron-impact ionization of rubidium. As expected, first-order plane-wave models for the projectile are inadequate to describe our experimental data, even for the relatively small scattering angles of $-15°$ and $-20°$. The best agreement with experiment is obtained by using a fully nonperturbative model such as convergent close coupling (CCC), although differences between experiment and theory remain in both the relative height of the binary peaks and, more clearly, in the actual position of the peak. The origin of these remaining discrepancies is not known at present.

ACKNOWLEDGMENTS

This work was supported, in part, by the Australian Research Council (M.H., B.L., I.B.) and the Merit Allocation Scheme on the National Facility of the Australian Partnership for Advanced Computing (I.B.), and by the National Science Foundation (U.S.) (K.B.).

[1] I. E. McCarthy and E. Weigold, Rep. Prog. Phys. **54**, 789 (1991).
[2] L. Frost and E. Weigold, J. Phys. B **15**, 2531 (1982).
[3] M. Streun, G. Baum, W. Blask, J. Rasch, I. Bray, D. V. Fursa, S. Jones, D. H. Madison, H. R. J. Walters, and C. T. Whelan, J. Phys. B **31**, 4401 (1998).
[4] J. Lower, A. Elliot, E. Weigold, S. Mazevet, and J. Berakdar, Phys. Rev. A **62**, 012706 (2000).
[5] M. A. Haynes and B. Lohmann, J. Phys. B **33**, 4711 (2000).
[6] I. Bray, Phys. Rev. A **49**, 1066 (1994).
[7] V. Karaganov, I. Bray, and P. J. O. Teubner, J. Phys. B **31**, L187 (1998).
[8] K. A. Stockman, V. Karaganov, I. Bray, and P. J. O. Teubner, J. Phys. B **34**, L187 (2001).
[9] B. V. Hall, Y. Shen, A. J. Murray, M. C. Standage, W. R. MacGillivray, and I. Bray, J. Phys. B **37**, 1113 (2004).
[10] I. Bray and D. V. Fursa, Phys. Rev. A **54**, 2991 (1996).
[11] I. Bray, Phys. Rev. Lett. **89**, 273201 (2002).
[12] I. Bray, Phys. Rev. Lett. **78**, 4721 (1997).
[13] I. Bray, J. Phys. B **36**, 2203 (2002).
[14] K. Bartschat and P. G. Burke, J. Phys. B **20**, 3191 (1987).
[15] K. Bartschat, Comput. Phys. Commun. **75**, 219 (1993).
[16] R. H. G. Reid, K. Bartschat, and A. Raeker, J. Phys. B **31**, 563 (1998); **33**, 5261 (2000).
[17] Y. Fang and K. Bartschat, J. Phys. B **34**, L19 (2001).